Electronic Supplementary Material (ESI) for Journal of Materials Chemistry A.

Supporting information

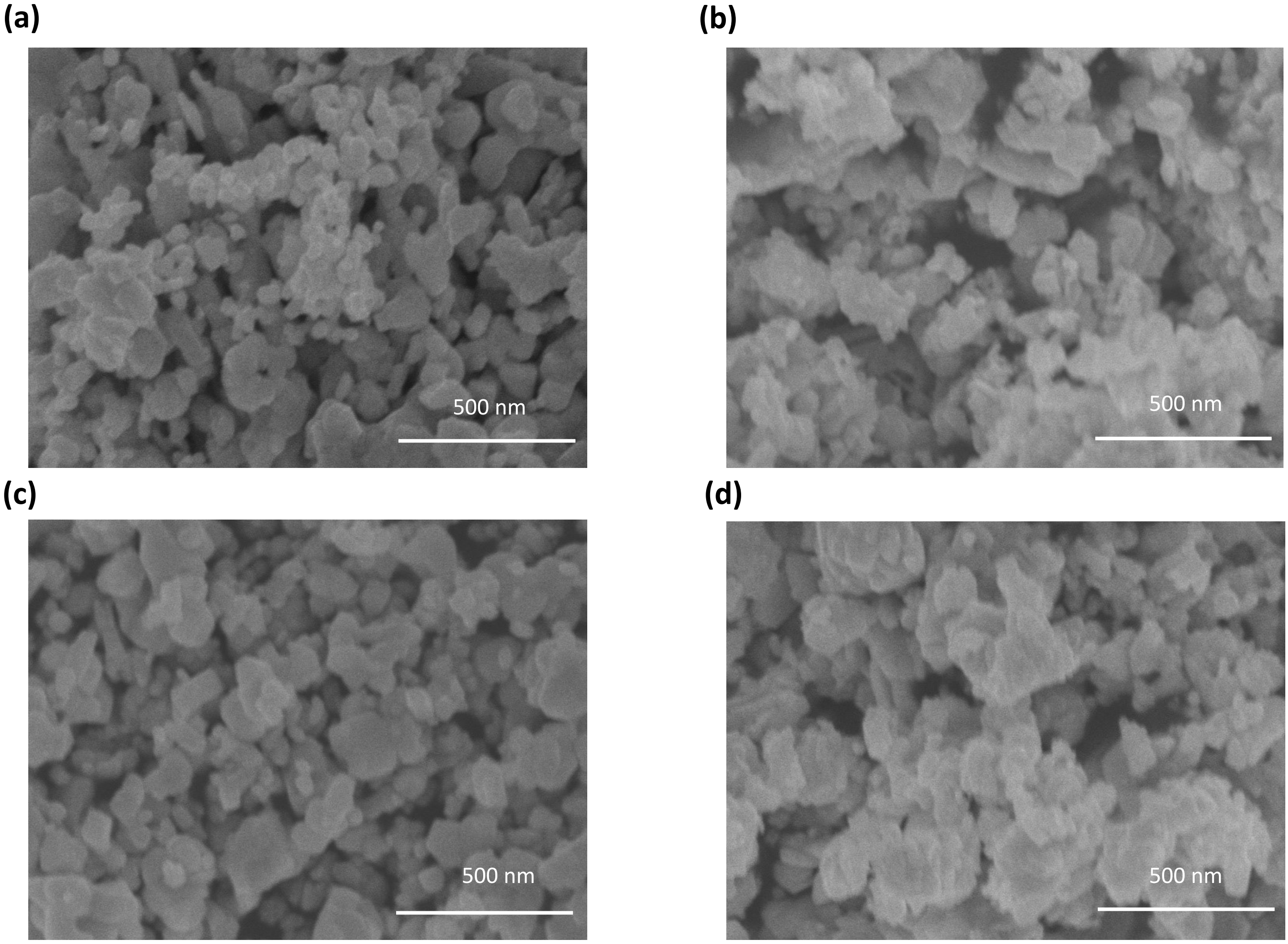

Fig. S1 SEM images of $BaTaO_2N$ prepared using nitridation temperatures and durations of (a) 1073 K/15 h, (b) 1173 K/2 h, (c) 1173 K/10 h, and 1273 K/0.5 h.

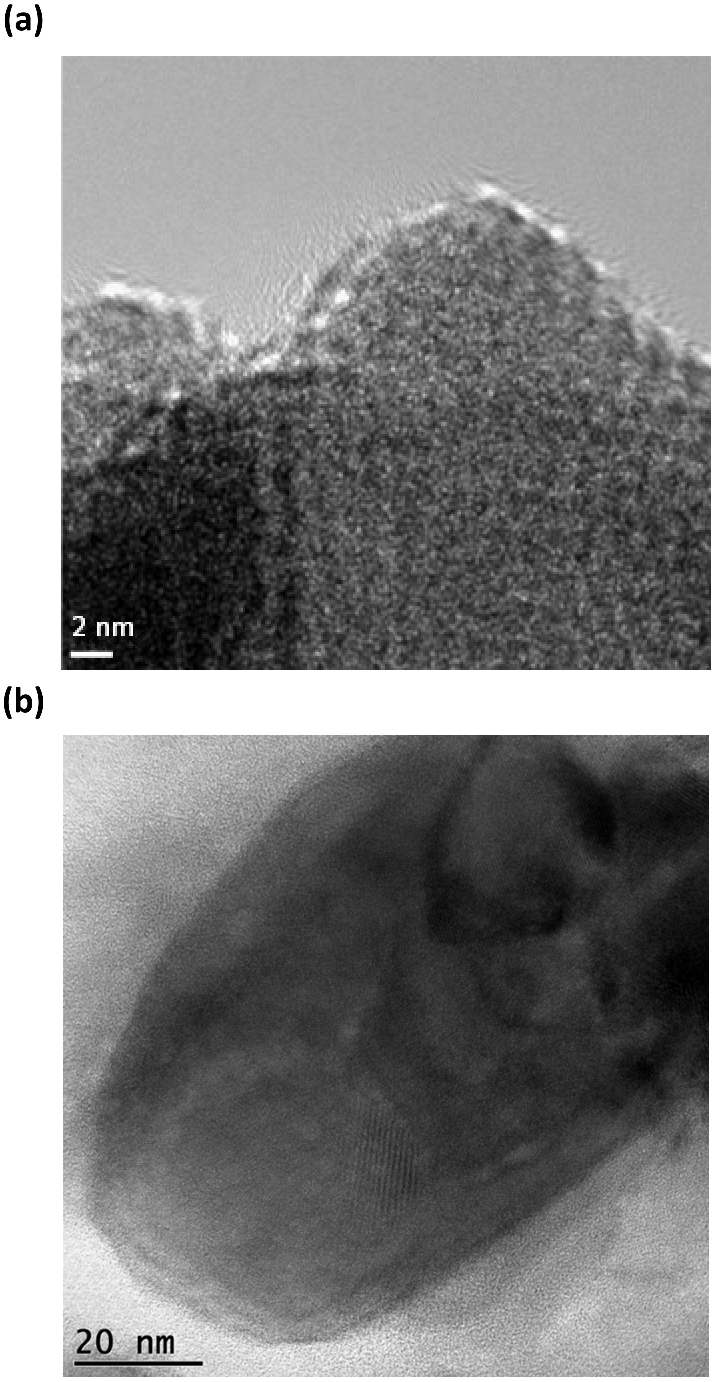

Fig. S2 High-resolution transmission electron spectroscopy images (HR-TEM) of (a) a-Ta_2O_5 and (b) $BaTaO_2N$. $BaTaO_2N$ was prepared from a mixture of $BaCO_3$ and a-Ta_2O_5 by NH_3 nitridation at 1123 K for 5 h.

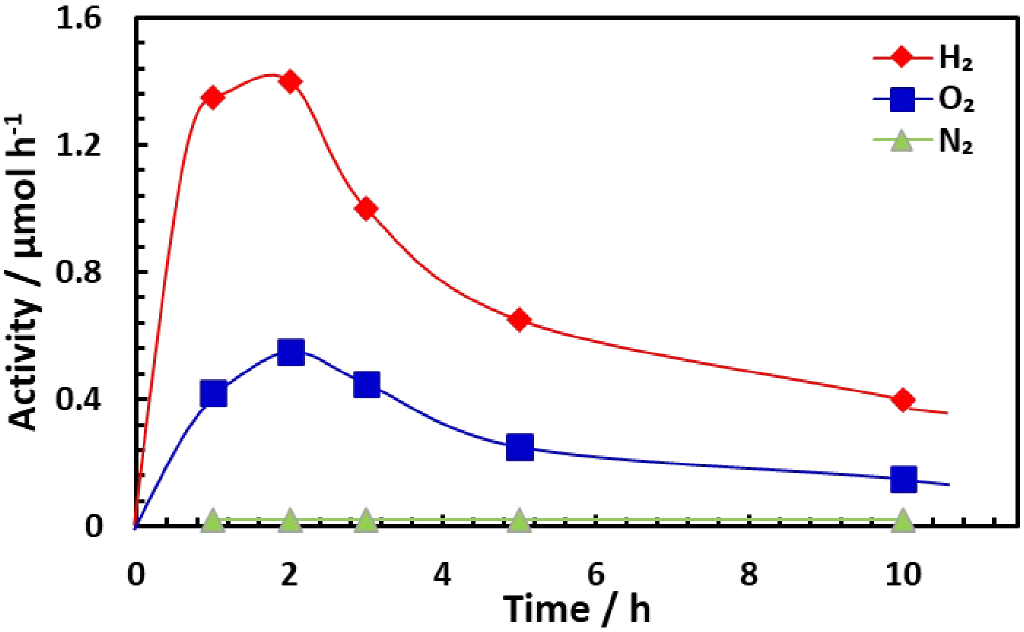

Fig. S3 Effects of nitridation time on the photocatalytic activity of $BaTaO_2N$ during the water splitting reaction. The $BaTaO_2N$ was prepared by nitridation at 1173 K for varying durations and was loaded with 4 wt% Rh, 0.5 wt% Cr_2O_3 and 0.3 wt% IrO_2 as cocatalysts. Reaction conditions: lamp source; 300 W Xe lamp (λ>420 nm), reaction temperature; 288 K, background pressure; Ar at 5 kPa.

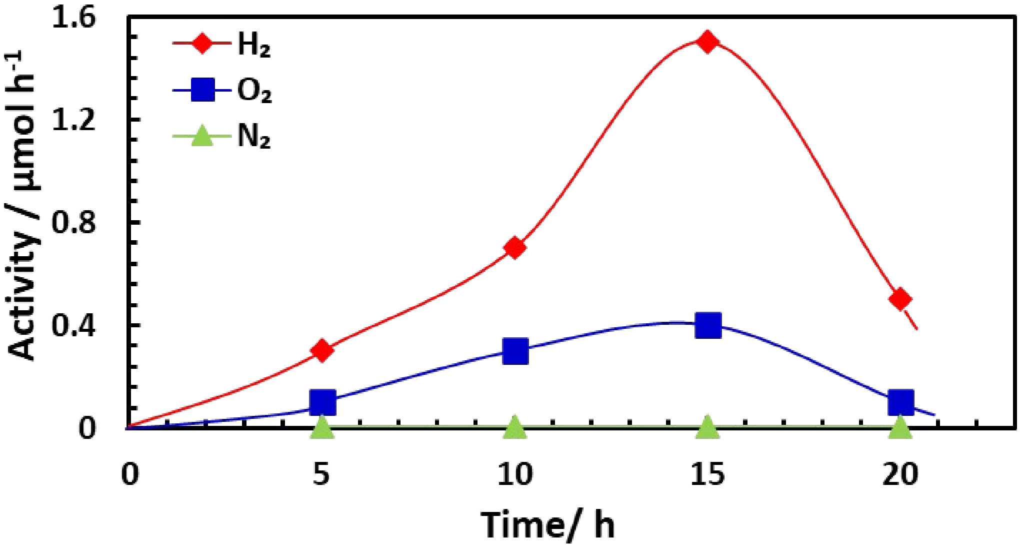

Fig. S4 Effects of nitridation time on the photocatalytic activity of $BaTaO_2N$ during the water splitting reaction. The $BaTaO_2N$ was prepared by nitridation at 1073 K for varying durations and was loaded with 4 wt% Rh, 0.5 wt% Cr_2O_3 and 0.3 wt% IrO_2 as cocatalysts. Reaction conditions: lamp source; 300 W Xe lamp (λ>420 nm), reaction temperature; 288 K, background pressure; Ar at 5 kPa.

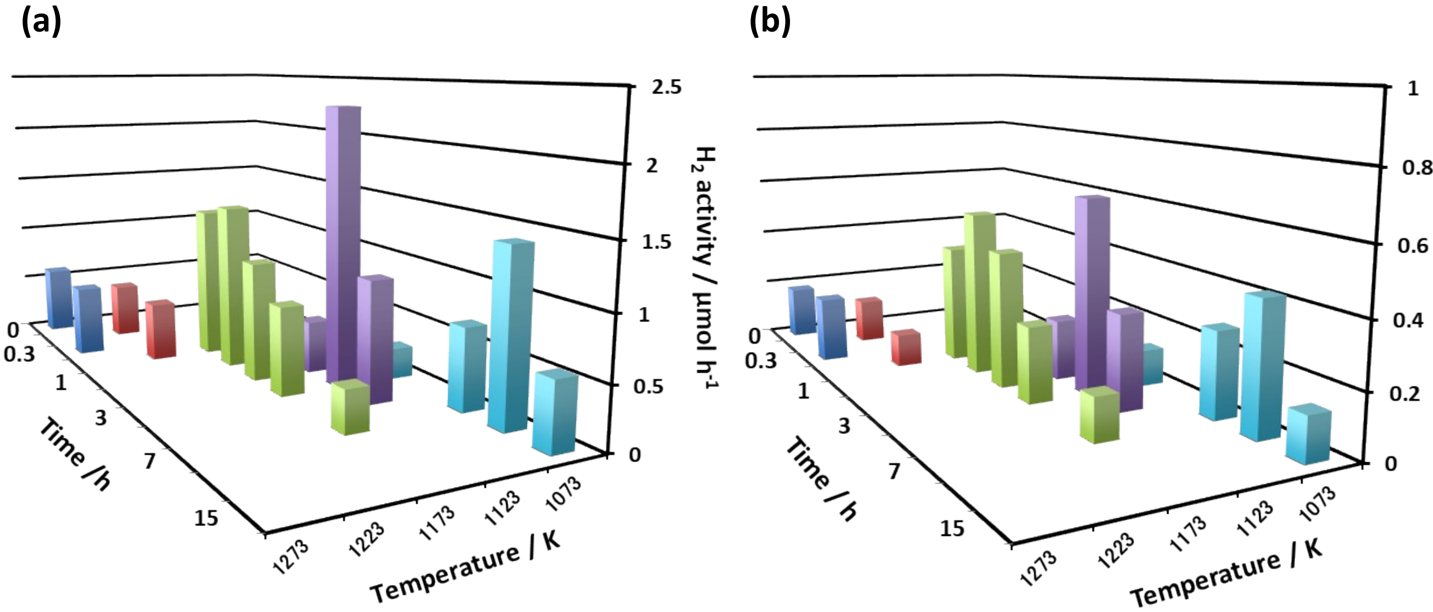

Fig. S5 Three-dimensional representations of photocatalytic activity as reflected in (a) H_2 and (b) O_2 evolution as functions of nitridation temperature and duration. The $BaTaO_2N$ was prepared by nitridation at 1073 to 1273 K for 0.5 to 20 h and was loaded with 4 wt% Rh, 0.5 wt% Cr_2O_3 and 0.3 wt% IrO_2 as cocatalysts. Reaction conditions: lamp source; 300 W Xe lamp (λ>420 nm), reaction temperature; 288 K, background pressure; Ar at 5 kPa.

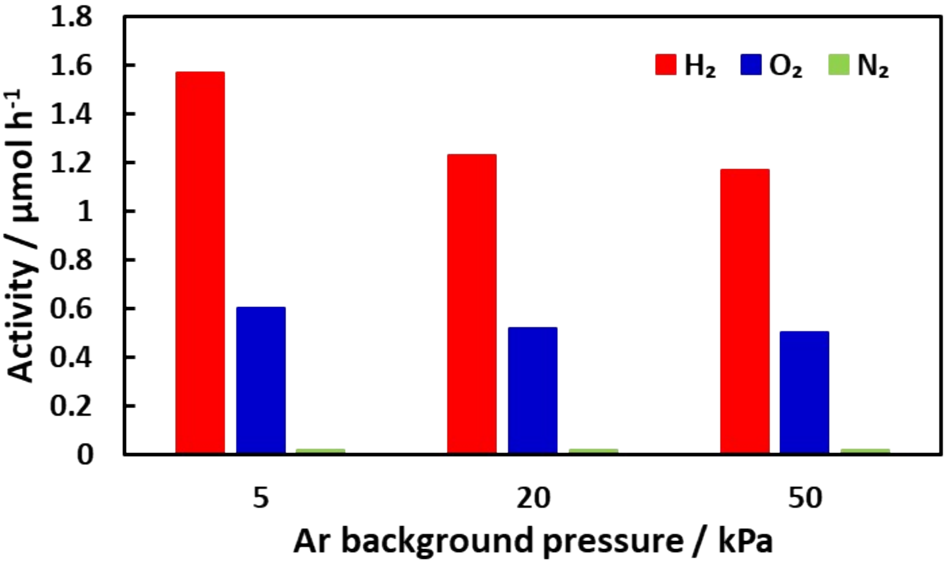

Fig. S6 Effects of the background Ar gas pressure on the photocatalytic activity of Rh/Cr_2O_3/IrO_2-loaded $BaTaO_2N$. The $BaTaO_2N$ was prepared by nitridation at 1123 K for 5 h and was loaded with 2 wt% Rh, 1 wt% Cr_2O_3 and 0.3 wt% IrO_2 as cocatalysts. Reaction conditions: lamp source; 300 W Xe lamp (λ>420 nm), reaction temperature; 288 K.

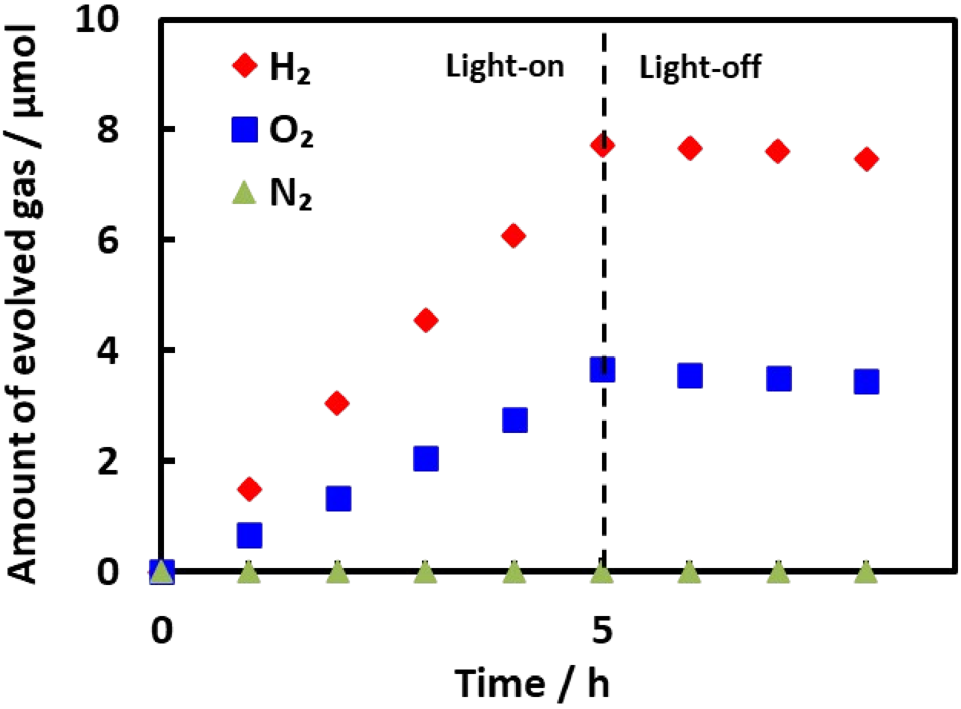

Fig.S7 Changes in the amounts of H_2 and O_2 in the gas phase during light irradiation and dark(light-off). The $BaTaO_2N$ was prepared by nitridation at 1123 K for 5 h and was loaded with 2 wt% Rh, 1 wt% Cr_2O_3 and 0.3 wt% IrO_2 as cocatalysts. Reaction conditions: lamp source; 300 W Xe lamp (λ>420 nm), reaction temperature; 288 K, background pressure; Ar at 5 kPa.

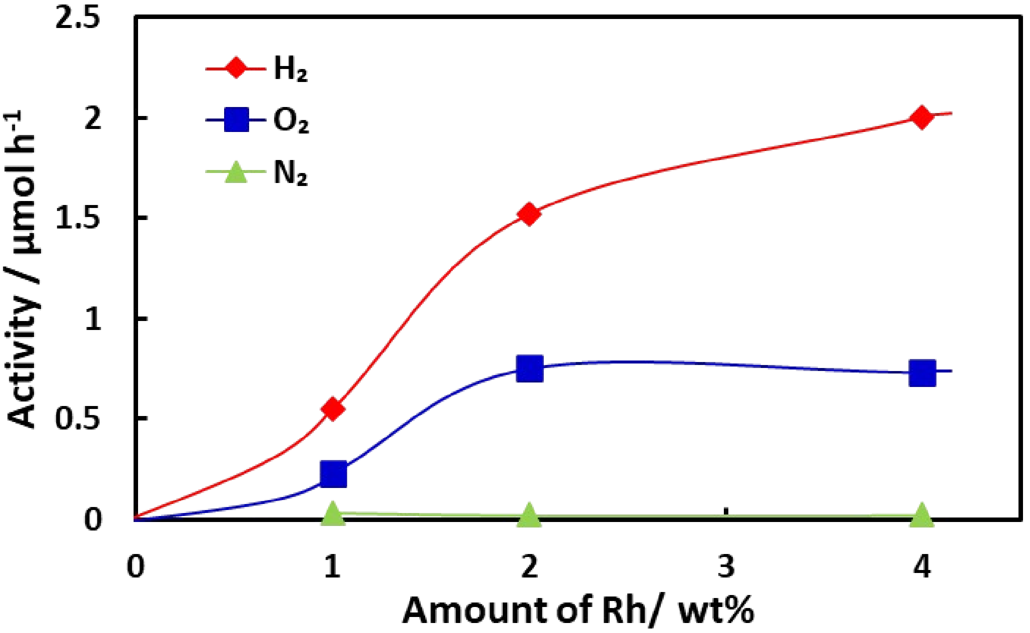

Fig. S8 Effects of the extent of Rh loading on the photocatalytic activity of Rh/Cr_2O_3/IrO_2-loaded $BaTaO_2N$. The $BaTaO_2N$ was prepared by nitridation at 1123 K for 5 h and was loaded with 1-4 wt% Rh, 0.5 wt% Cr_2O_3 and 0.3 wt% IrO_2 as cocatalysts. Reaction conditions: lamp source; 300 W Xe lamp (λ>420 nm), reaction temperature; 288 K, background pressure; Ar at 5 kPa.

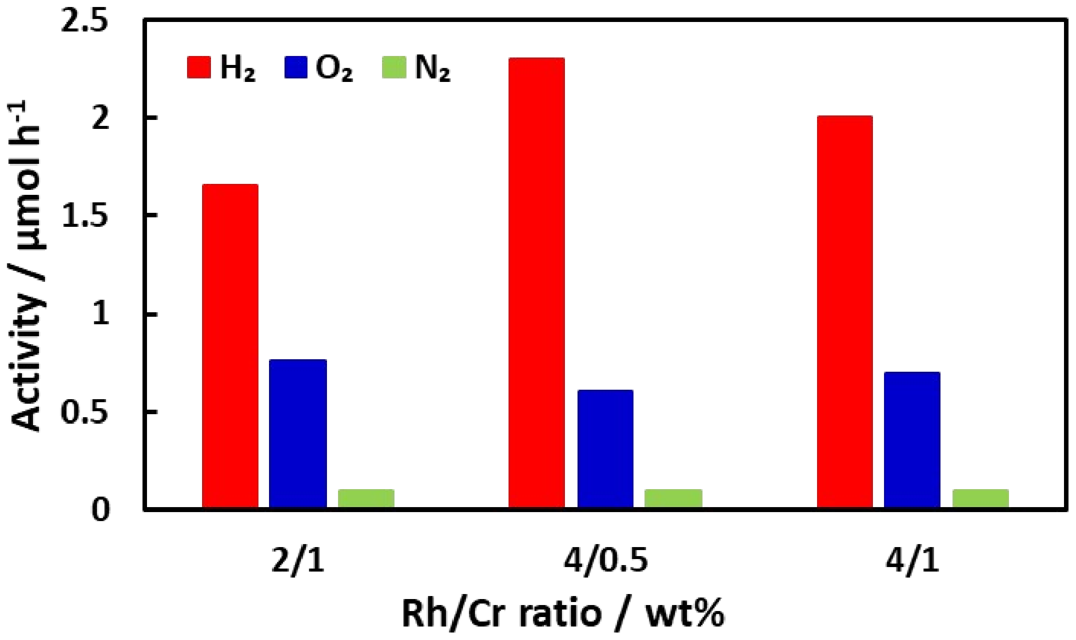

Fig. S9 The effects of the Rh/Cr ratio on the photocatalytic activity of $Rh/Cr_2O_3/IrO_2$-loaded $BaTaO_2N$. The $BaTaO_2N$ was prepared by nitridation at 1123 K for 5 h and was loaded with 2 or 4 wt% Rh, 0.5 or 1.0 wt% Cr_2O_3 and 0.3 wt% IrO_2 as cocatalysts. Reaction conditions: lamp source; 300 W Xe lamp (λ>420 nm), reaction temperature; 288 K, background pressure; Ar at 5 kPa.

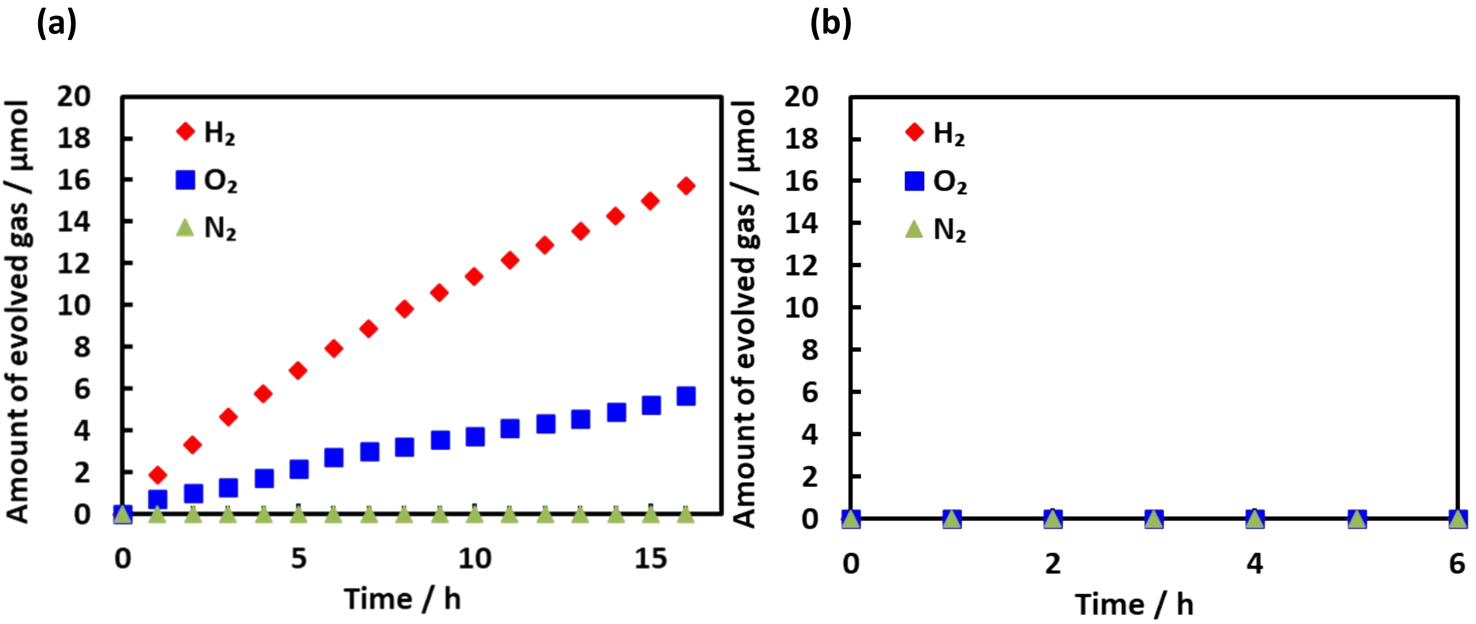

Fig. S10 Water splitting reaction on (a) Rh/Cr_2O_3-loaded and (b) IrO_2-loaded $BaTaO_2N$. The $BaTaO_2N$ was prepared by nitridation at 1123 K for 5 h and was loaded with 2 wt% Rh, 1 wt% Cr_2O_3 and 0.3 wt% IrO_2 as cocatalysts. Reaction conditions: lamp source; 300 W Xe lamp (λ>420 nm), reaction temperature; 288 K, background pressure; Ar at 5 kPa.

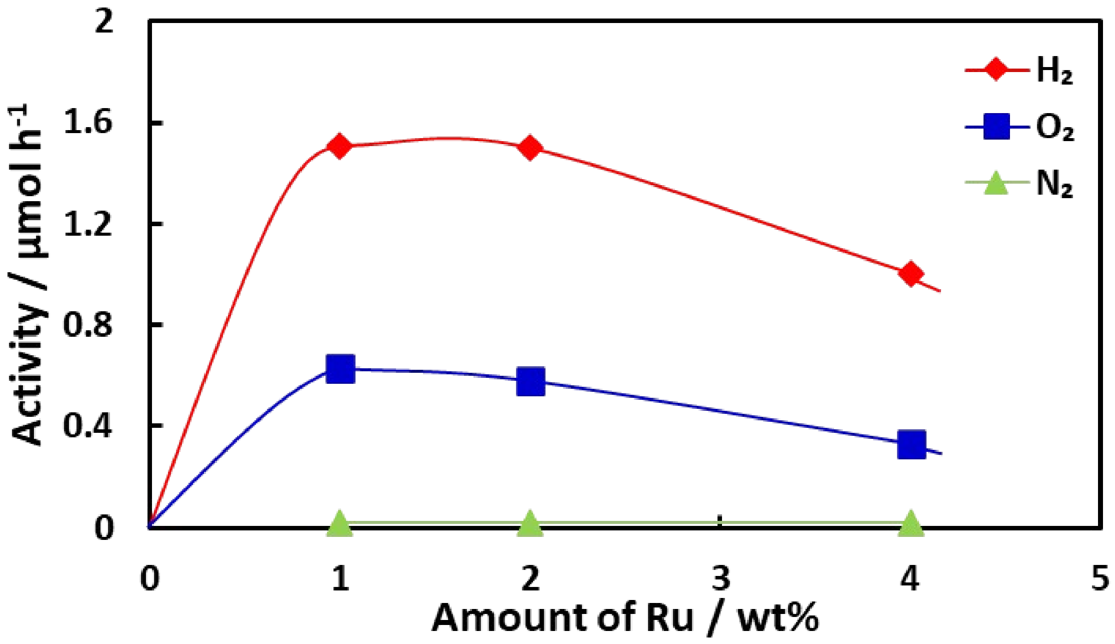

Fig. S11 Variations in the photocatalytic activity of Ru/Cr_2O_3/IrO_2-loaded $BaTaO_2N$ with changes in Ru loading. The $BaTaO_2N$ was prepared by nitridation at 1123 K for 5 h and was loaded with 1-4 wt% Ru, 1 wt% Cr_2O_3 and 0.3 wt% IrO_2 as cocatalysts. Reaction conditions: lamp source; 300 W Xe lamp (λ>420 nm), reaction temperature; 288 K, background pressure; Ar at 5 kPa.

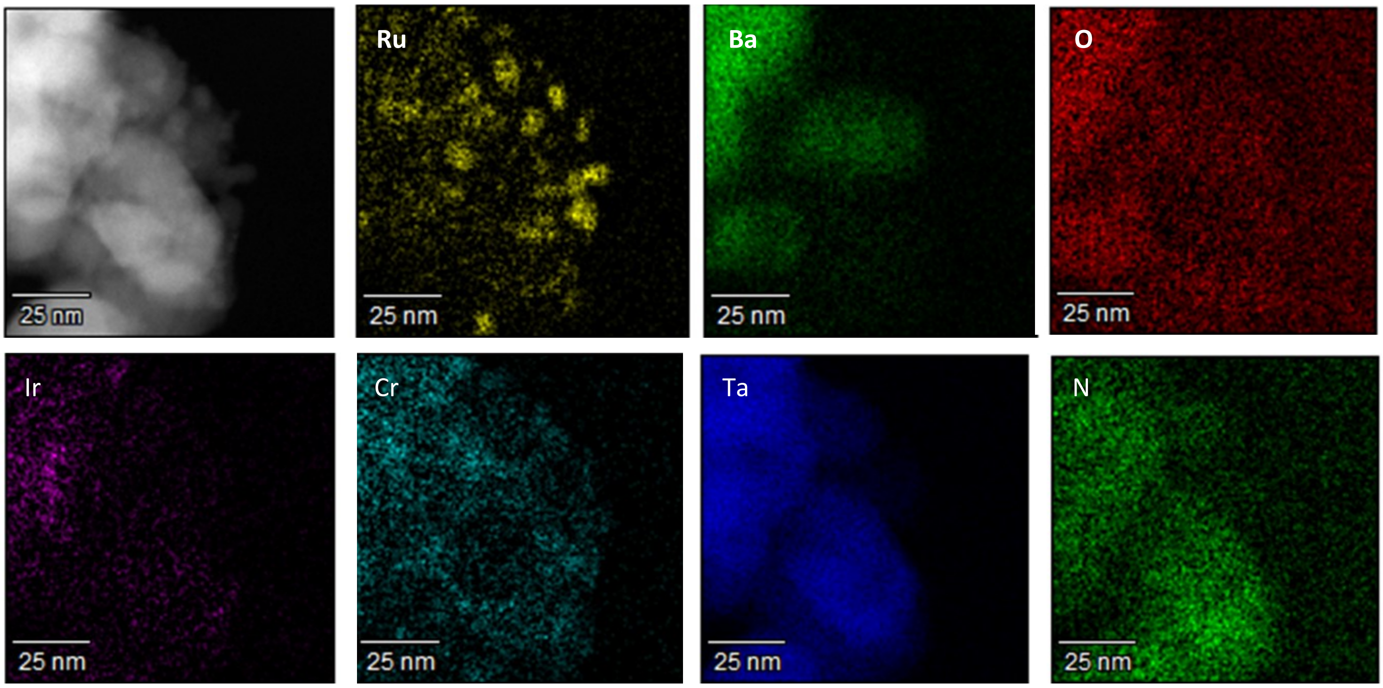

Fig. S12 Annular dark-field STEM images and STEM-EDS elemental maps of Ru/Cr_2O_3/IrO_2-$BaTaO_2N$. The $BaTaO_2N$ was prepared by nitridation at 1123 K for 5 h and was loaded with Ru/Cr_2O_3/IrO_2 at 2/1/0.3 wt%.

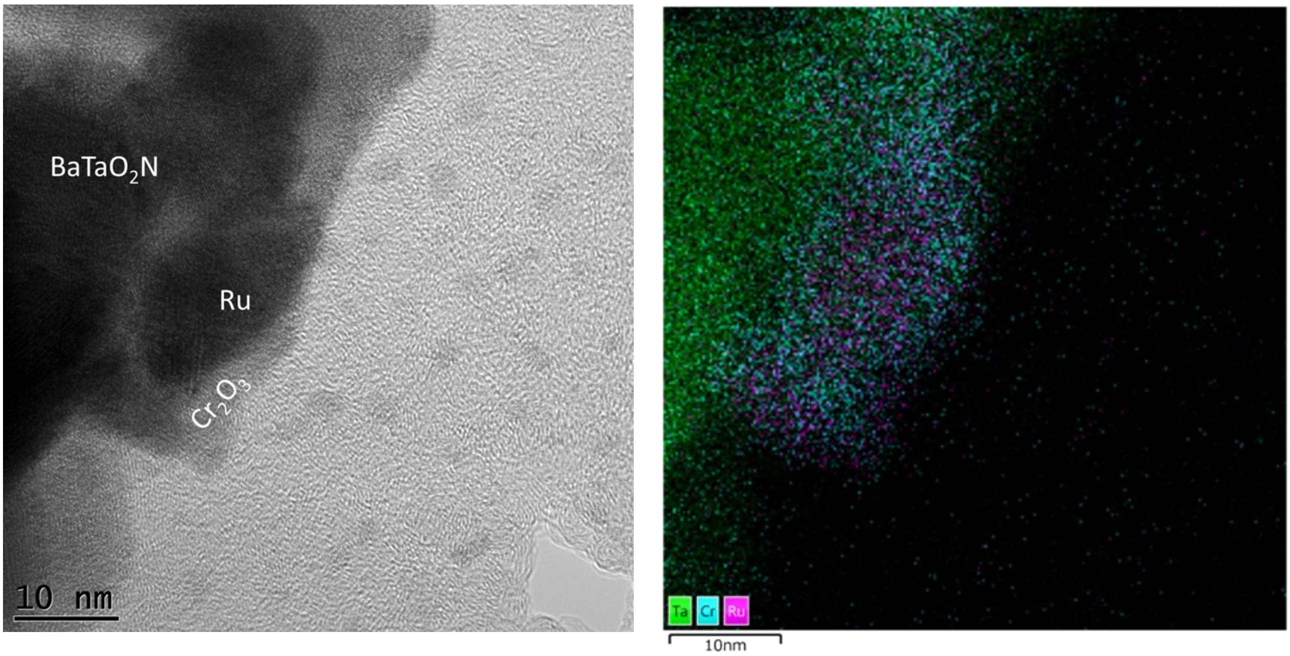

Fig. S13 A high resolution transmission electron spectroscopy (HR-TEM) image of BaTaO$_2$N and its EDS mapping. Color: magenta, blue and green show Ru, Cr and Ta, respectively.

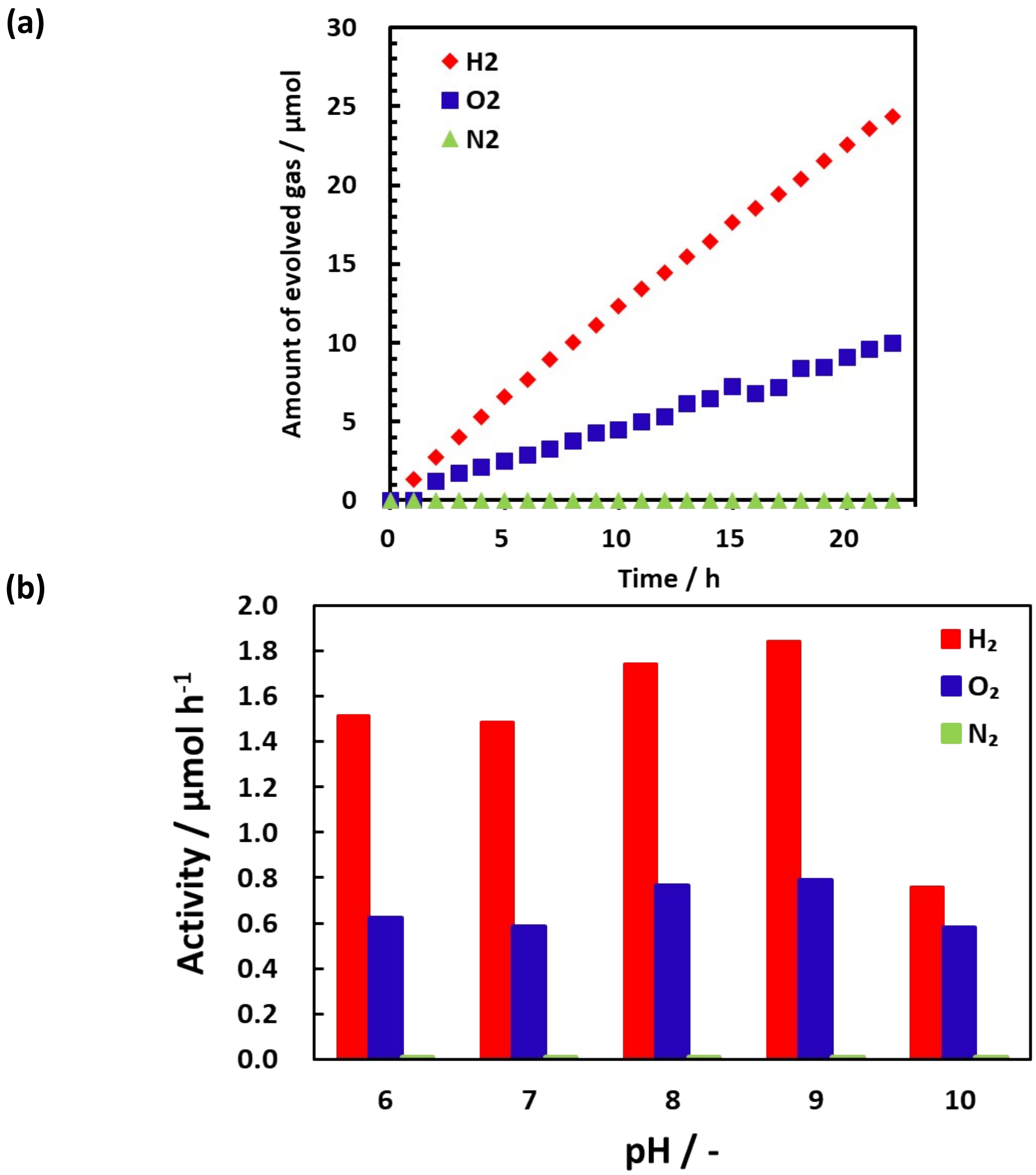

Fig. S14 (a) Evolution of gaseous products during the water splitting reaction on Rh-loaded $BaTaO_2N$ in an aqueous K_2CrO_4 solution and (b) the effects of pH on the photocatalytic activity. The $BaTaO_2N$ was prepared by nitridation at 1123 K for 5 h and was loaded with 2 wt% Rh. Reaction conditions: 0.22 mM aqueous K_2CrO_4 solution, pH; adjusted by adding NaOH and HCl, lamp source; 300 W Xe lamp (λ>420 nm), reaction temperature; 288 K, background pressure; Ar at 5 kPa.

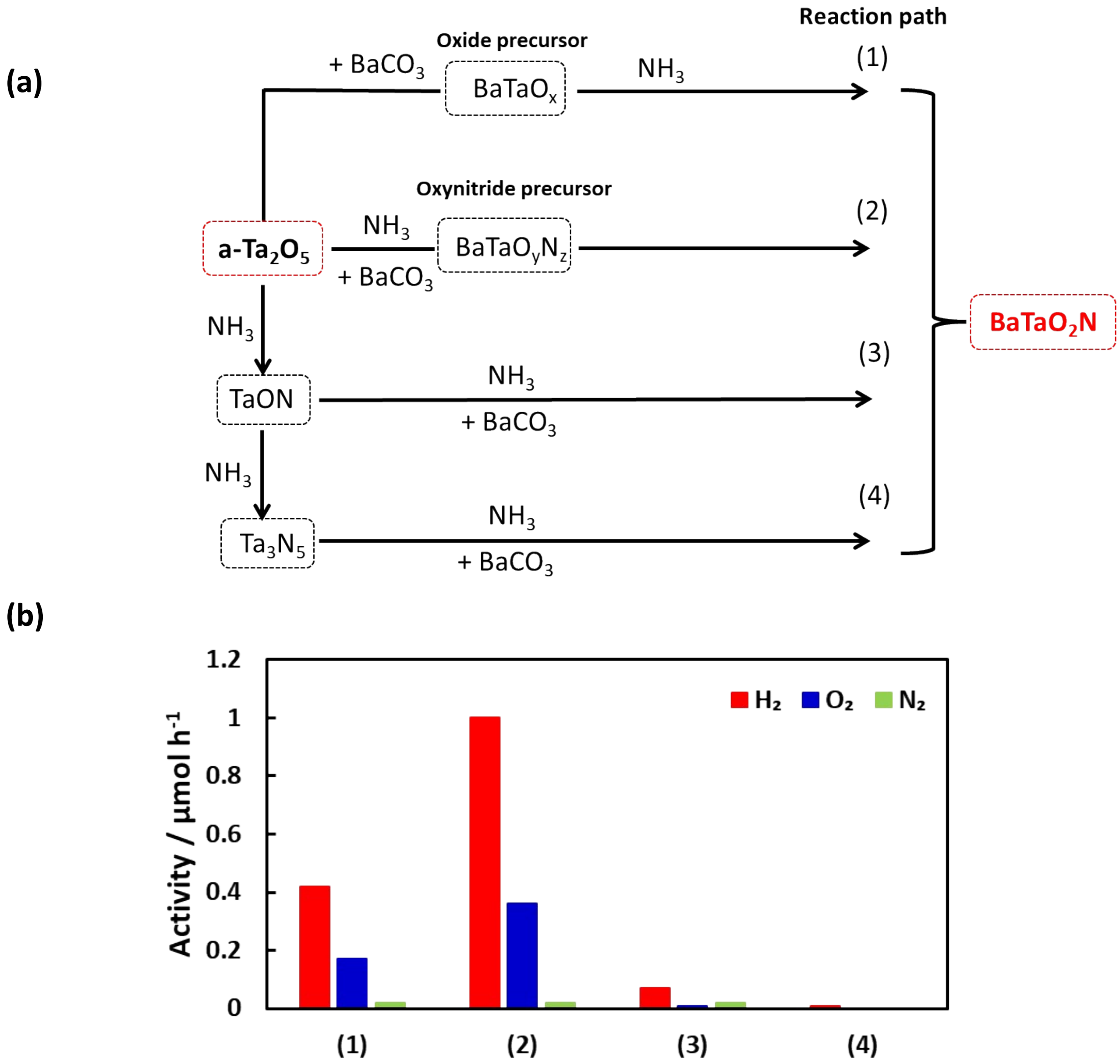

Fig. S15 (a) Schematic representation of the possible reactions involved in BaTaO$_2$N formation from a mixture of BaCO$_3$ and a-Ta$_2$O$_5$ in a flow of NH$_3$ and (b) the photocatalytic activities during the water splitting reaction of BaTaO$_2$N synthesized via the various paths. Reaction path (1): the oxide precursor BaTaO$_x$ was first prepared by the reaction of BaCO$_3$ with a-Ta$_2$O$_5$ in air at 1173 K for 1 h. The XRD pattern for the product showed broad peaks attributed to amorphous Ba$_5$Ta$_4$O$_{15}$. An NH$_3$-based nitridation was subsequently carried out at 1173 K for 2 h to obtain BaTaO$_2$N. Reaction path (2): the oxynitride precursor BaTaO$_x$N$_y$ was first prepared by the pre-reaction of BaCO$_3$ with a-Ta$_2$O$_5$ in a flow of NH$_3$ at 993 K for 1 h, followed by further NH_3 nitridation at 1173 K for 1 h. Reaction path (3): TaON was prepared from a-Ta_2O_5 by nitridation in a flow of NH_3 (flow rate of 40 mL min^{-1}) at 1173 K for 1 h. The reaction of $BaCO_3$ with TaON was then performed in NH_3 at 1173 K for 1 h. Reaction path (4): Ta_3N_5 was prepared from a-Ta_2O_5 by nitridation in a flow of NH_3 (flow rate of 70 mL min^{-1}) at 1173 K for 3 h. The reaction of Ta_3N_5 with $BaCO_3$ to produce $BaTaO_2N$ was then carried out in a N_2 atmosphere at 1173 K for 1 h. The activity during the water splitting reaction was examined after loading IrO_2 (0.3 wt%), Cr_2O_3 (0.5 wt%) and Rh (4 wt%) as cocatalysts. Reaction conditions; lamp source; 300 W Xe lamp, wavelength of illuminated light; λ>420 nm, reaction temperature; 288 K, background pressure; Ar at 5 kPa.

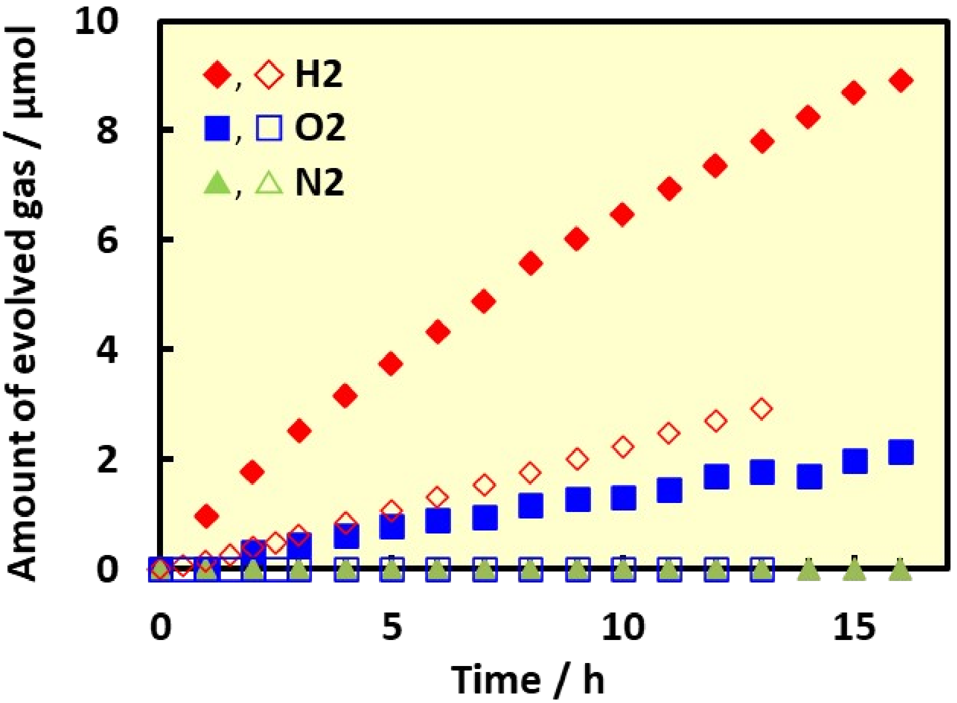

Fig. S16 Effects of oxidation on the activity of $BaTaO_2N$ deactivated by prolonged NH_3 nitridation. ◊, □: Before oxidation, ♦, ■: After oxidation. The $BaTaO_2N$ was prepared by nitridation in a flow of NH_3 at 1123 K for 15 h. Oxidation was carried out by exposure to N_2 containing O_2 (100 ppm) at 823 K for 2 h. Cocatalysts: Rh at 4 wt%, Cr_2O_3 at 1.0 wt% and IrO_2 at 0.3 wt%. Reaction conditions: lamp source; 300 W Xe lamp, wavelength of illuminated light; λ>420 nm, reaction temperature; 288 K, background pressure; Ar at 5 kPa.

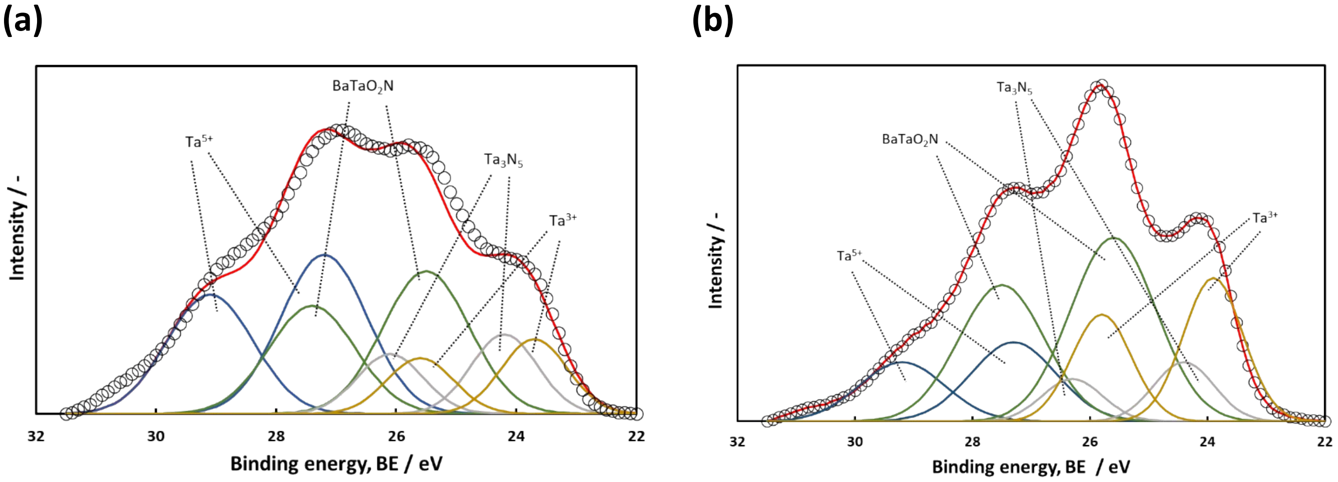

Fig. S17 Ta 4f X-ray photoelectron spectra obtained for $BaTaO_2N$ prepared at 1123 K for (a) 5 and (b) 20 h. The Ta 4f peaks showed very complicated shapes that could be assigned to Ta $4f_{7/2}$ and $Ta_{5/2}$ contributions. Since both the 5 and 20 h specimens contained small amounts of Ta_3N_5, the contribution of this phase to the Ta 4f signals was considered. Curve fitting of the Ta 4f signals was difficult in the case of $BaTaO_2N$ and so a precursor oxynitride such as $BaTaO_xN_y$ was assumed to be present in addition to $BaTaO_2N$. The solid lines indicate that a combination of Ta 4f signals due to $BaTaO_2N$, $BaTaO_xN_y$ and Ta_3N_5 was in good agreement with the experimental signal shape in the binding energy region higher than 25 eV, below which contributions by Ta^{3+} were indicated. The Ta $4f_{7/2}$ (Ta $4f_{5/2}$) binding energy values were 25.7±0.1 eV (27.6±0.1 eV) for $BaTaO_2N$, 27.2±0.1 eV (29.1±0.1 eV) for $BaTaO_xN_y$, 24.5±0.05 eV (26.4±0.05 eV) for Ta_3N_5 and 23.8±0.2 eV (25.7±0.2 eV) for Ta^{3+}.

Table S1 The proportions of various components identified in $BaTaO_2N$ samples nitrided for 3, 5 and 20 h.

Nitridation time / h	Ta^{5+} ($BaTaO_2N$)	Ta^{5+} ($BaTaO_xN_y$)	Ta^{5+} (Ta_3N_5)	Ta^{3+}
3	0.30	0.48	0.13	0.10
5	0.35	0.39	0.13	0.13
20	0.43	0.20	0.11	0.27

With increasing nitridation duration, the proportion of the Ta 4f signal due to $BaTaO_xN_y$ decreased while that related to $BaTaO_2N$ increased. This change was consistent with the assumption that $BaTaO_xN_y$ was present. It should be noted that the proportion of Ta^{3+} was much higher in the $BaTaO_2N$ specimen nitrided for 20 h compared with the 5 h sample.